

# Quadrupole Shifts for the $^{171}\text{Yb}^+$ Ion Clocks: Experiments versus Theories

D. K. Nandy and B. K. Sahoo

*Theoretical Physics Division, Physical Research Laboratory, Ahmedabad-380009, India and  
Indian Institute of Technology Gandhinagar, Ahmedabad, India\**

(Dated: Received date; Accepted date)

Quadrupole shifts for three prominent clock transitions,  $[4f^{14}6s]^2S_{1/2} \rightarrow [4f^{14}5d]^2D_{3/2}$ ,  $[4f^{14}6s]^2S_{1/2} \rightarrow [4f^{14}5d]^2D_{5/2}$  and  $[4f^{14}6s]^2S_{1/2} \rightarrow [4f^{13}6s^2]^2F_{7/2}$ , in the  $\text{Yb}^+$  ion are investigated by calculating quadrupole moments ( $\Theta$ s) of the  $5d_{3/2,5/2}$  and  $4f_{7/2}$  states using the relativistic coupled-cluster (RCC) methods. We find an order difference in the  $\Theta$  value of the  $4f_{7/2}$  state between our calculation and the experimental result, but our result concur with the other calculations that are carried out using different many-body methods than ours. Nevertheless, our  $\Theta$  value of the  $5d_{3/2}$  state is in good agreement with the available experimental result and becomes more precise till date estimating the quadrupole shift of the  $[4f^{14}6s]^2S_{1/2} \rightarrow [4f^{14}5d]^2D_{3/2}$  clock transition more accurately. To justify accuracies in our calculations, we also evaluate the hyperfine structure constants of the  $6s_{1/2}$ ,  $5d_{3/2,5/2}$  and  $4f_{7/2,5/2}$  states of  $^{171}\text{Yb}^+$  ion using the same RCC method and compare the results with their experimental values. Moreover, we determine lifetime of the  $5d_{3/2}$  state to eradicate disagreement on its value from two different experiments.

PACS numbers:

The single charged  $\text{Al}^+$  ion is the most accurate atomic clock till date [1], which proves that one of the singly charged ions is capable of becoming the primary frequency standard in future. Few more successful optical single ion clocks are  $\text{Hg}^+$  [2],  $\text{Ca}^+$  [3],  $\text{Sr}^+$  [4],  $\text{Yb}^+$  [5, 6] etc. In  $\text{Yb}^+$ , two quadrupole (E2)  $[4f^{14}6s]^2S_{1/2} \rightarrow [4f^{14}5d]^2D_{3/2}$  and  $[4f^{14}6s]^2S_{1/2} \rightarrow [4f^{14}5d]^2D_{5/2}$  transitions having optical wavelengths 436 nm and 411 nm, respectively and an octupole (E3)  $[4f^{14}6s]^2S_{1/2} \rightarrow [4f^{13}6s^2]^2F_{7/2}$  transition with optical wavelength 467 nm are considered for the clock measurements, see schematic diagram in Fig. 1, in many laboratories around the globe [5–8]. Since the field-induced frequency shifts in the  $[4f^{13}6s^2]^2F_{7/2}$  state is very low and it is also highly meta-stable [9], it makes the above octupole transition as an instinctive choice for the most precise next generation optical clock. Although lifetime of the  $[4f^{13}6s^2]^2F_{7/2}$  state is very long ( $> 6$  years) which cannot be considered as interrogation time during the clock frequency measurement, instead its probe interaction time ( $\sim 10$  s) serves for this purpose [9]. On the otherhand, lifetimes of the metastable  $[4f^{14}5d]^2D_{3/2}$  and  $[4f^{14}5d]^2D_{5/2}$  states are about 55 ms and 7 ms, respectively [10, 11] and can be used as interrogation times in the clock transitions involving these states. Owing to these facts, many other important studies like parity nonconservation [12, 13], quantum information [14], variation of the fine structure constant [15] etc. using the above transitions in  $\text{Yb}^+$  are also in progress.

One of the major resources that contribute to the uncertainty budget of a clock frequency measurement is the quadrupole shift due to the stray electric field gradient present in the experiment [16]. This shift can be accurately estimated with precise knowledge of the quadrupole moments ( $\Theta$ s) of the states involved in a clock transition. This urges for determination of  $\Theta$ s for the

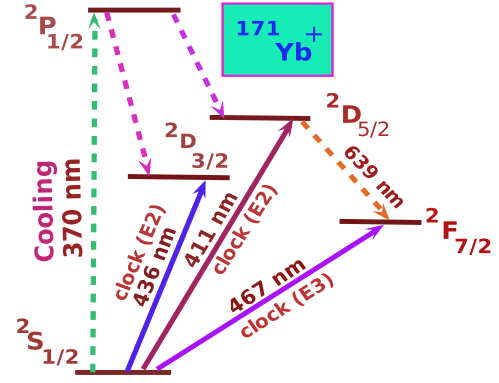


FIG. 1: (color online) Schematic view of the energy levels and the clock transitions in the  $^{171}\text{Yb}^+$  ion.

$[4f^{14}5d]^2D_{3/2}$ ,  $[4f^{14}5d]^2D_{5/2}$  and  $[4f^{13}6s^2]^2F_{7/2}$  states ( $\Theta$  of the  $[4f^{14}6s]^2S_{1/2}$  is zero as  $J = 0$ ) of  $\text{Yb}^+$  as accurately as possible. In an experiment,  $\Theta$  is measured by altering static direct current (dc) voltage. A theoretical study on this property is indispensable for three important rationale: (i) when the experimental results are not available, the calculated values can be helpful to estimate the quadrupole shifts, (ii) it can prevent performing auxiliary measurements for the atomic clock experiments which are very expensive and (iii) comparison between the measurement and a calculation serves as a tool to test the potential of the employed many-body method. The previous calculations for  $\Theta$ s in  $\text{Yb}^+$  are reported as  $2.174 ea_0^2$  [17] and  $2.157 ea_0^2$  [18] against the measured value  $2.08(11) ea_0^2$  [19] for the  $[4f^{14}5d]^2D_{3/2}$  state and for the  $[4f^{13}6s^2]^2F_{7/2}$  state the calculations give values as  $-0.22 ea_0^2$  [20] and  $-0.20 ea_0^2$  [21] compared to a small experimental result  $-0.041(5)ea_0^2$  [9]. The calculations reported by Latha et al. [18] employ

the relativistic coupled-cluster (RCC) method while calculations by Itano [17] has been carried out using a multi-configuration Dirac-Fock (MCDF) method. For the  $[4f^{13}6s^2]^2F_{7/2}$  state, Blythe et al. [20] had employed the MCDF method, while Porsev et al. [21] have carried out these calculations inconclusively using a CI method and roughly estimating this quantity as  $\sim -0.1 \text{ } ea_0^2$ . In this Letter, we intend to perform calculations of  $\Theta$ s in the above states including their fine structure partners  $[4f^{14}5d]^2D_{5/2}$  and  $[4f^{13}6s^2]^2F_{5/2}$  states considering all possible configurations within the singles and doubles approximation in our recently developed [22, 23] RCC (CCSD) methods, which are more accurate than the CI or MCDF methods at the same level of truncation [24, 25], to comprehend the role of the electron correlation effects better and to elucidate plausible reasons for the discrepancies between the above theoretical and experimental  $\Theta$  values. In addition, we also calculate the magnetic dipole hyperfine constants ( $A_{hf}$ s) of the above states of  $^{171}\text{Yb}^+$  and compare them against their experimental values to gain insights into the accuracies of our calculations. We also determine lifetime of the  $[4f^{14}5d]^2D_{3/2}$  state to eradicate a conflict between two different measured values [10, 11].

Theoretically quadrupole moment  $\Theta(\gamma F)$  of a hyperfine state,  $|(\gamma IJ)FM_F\rangle$ , with angular momentum  $F$  and azimuthal component  $M_F$  component for the nuclear angular momentum  $I$ , atomic angular momentum  $J$  and  $\gamma$  representing other additional additional information of the state is defined by  $\Theta(\gamma F) = \langle(\gamma IJ)FF|\Theta_0^{(2)}|(\gamma IJ)FF\rangle$  with  $\Theta_0^{(2)} = -\frac{\epsilon}{2} \sum_j (3z_j^2 - r_j^2)$ , the zeroth component of the quadrupole moment spherical tensor operator  $\Theta^{(2)}$  [30]. Using the Wigner-Eckart theorem, we can express [16]

$$\langle(\gamma IJ)FM_F|\Theta_q^{(2)}|(\gamma IJ)FM_F\rangle = (-1)^{F-M_F} \times \begin{pmatrix} F & 2 & F \\ M_F & q & -M_F \end{pmatrix} \times \langle F||\Theta^{(2)}||F\rangle, \quad (1)$$

where  $\langle F||\Theta_0^{(2)}||F\rangle$  is the reduced matrix element and in the  $IJ$ -coupling approximation given by

$$\langle F||\Theta^{(2)}||F\rangle = (-1)^{I+J+F}(2F+1) \begin{Bmatrix} J & 2 & J \\ F & I & F \end{Bmatrix} \times \begin{pmatrix} J & 2 & J \\ J & 0 & -J \end{pmatrix}^{-1} \Theta(\gamma J) \quad (2)$$

for  $\Theta(\gamma J) = \langle JJ|\Theta_0^{(2)}|JJ\rangle$  the quadrupole moment of the atomic state. The quadrupole shift ( $h\delta\nu_Q$ ) in the  $|(\gamma IJ)FM_F\rangle$  state due to the interaction Hamiltonian  $H_Q = \nabla \mathbf{E}^{(2)} \cdot \Theta^{(2)} = \sum_{q=-2}^2 (-1)^q \nabla E_q^{(2)} \Theta_{-q}^{(2)}$  with  $\nabla \mathbf{E}^{(2)}$  the electric field gradient is given by [16, 31]

$$h\delta\nu_Q = \frac{-2[3M_F^2 - F(F+1)]A\langle F||\Theta^{(2)}||F\rangle}{[(2F+3)(2F+2)2F(2F-1)]^{1/2}} \times [(3\cos^2\beta - 1) - \epsilon \sin^2\beta(\cos^2\alpha - \sin^2\alpha)], \quad (3)$$

where  $\alpha$  and  $\beta$  are the Euler angles used to convert from the principal-axis frame to the laboratory frame,  $\epsilon$  is known as the asymmetry parameter and  $A$  is known as the strength of the field gradient of the dc voltage.

Also, the  $A_{hf}$  of the  $|(\gamma IJ)FM_F\rangle$  state is given by [32]

$$A_{hf} = \mu_N g_I \frac{\langle J||T_e^{(1)}||J\rangle}{\sqrt{J(J+1)(2J+1)}} \quad (4)$$

where  $g_I$  and  $\mu_N$  are the gyromagnetic ratio and magnetic moment of the atomic nucleus and  $T_e^{(1)}$  is the even parity tensor of rank one representing the electronic component of the hyperfine interaction.

The lifetime of the  $[4f^{14}5d]^2D_{3/2}$  state ( $\tau_{5d3/2}$ ) of  $\text{Yb}^+$  can be determined as

$$\tau_{5d3/2} = \frac{1}{A_{5d3/2 \rightarrow 6s}^{M1} + A_{5d3/2 \rightarrow 6s}^{E2}}, \quad (5)$$

where  $A_{5d3/2 \rightarrow 6s}^{M1}$  and  $A_{5d3/2 \rightarrow 6s}^{E2}$  are the transition probabilities from the  $[4f^{14}5d]^2D_{3/2}$  state to the ground  $[4f^{14}6s]^2S_{1/2}$  state due to the magnetic dipole (M1) and electric quadrupole (E2) transitions, respectively.

We consider the Dirac-Coulomb (DC) Hamiltonian to calculate the atomic wave functions which is given in the atomic unit (au) by

$$H = \sum_i [c\alpha_D \cdot \mathbf{p}_i + (\beta_D - 1)c^2 + V_n(r_i) + \sum_{j \geq i} \frac{1}{r_{ij}}], \quad (6)$$

where  $\alpha_D$  and  $\beta_D$  are the Dirac matrices,  $c$  is the velocity of light and  $V_n(r)$  is the nuclear potential. The considered  $[4f^{14}6s^2]^2S_{1/2}$ ,  $[4f^{14}5d]^2D_{3/2,5/2}$  and  $[4f^{14}5d]^2D_{7/2,5/2}$  states have open-shell configurations, describing them using a common reference state function in the the Fock-space formalism of the RCC theory is strenuous. For this reason, we construct two reference states,  $|\Phi_0^{N-1}\rangle$  and  $|\Phi_0^{N+1}\rangle$ , using the Dirac-Fock (DF) method for the configurations  $[4f^{14}]$  and  $[4f^{14}6s^2]$ , respectively, with  $N = 69$  as the total number of occupied electrons of  $\text{Yb}^+$  targeting to calculate the wave functions for the above states. Here the  $[4f^{14}6s^2]^2S_{1/2}$  and  $[4f^{14}5d]^2D_{3/2,5/2}$  states can be determined using  $|\Phi_0^{N-1}\rangle$  (denoted by  $|\Psi_v\rangle$ ) and the  $[4f^{14}6s^2]^2S_{1/2}$  (again) and  $[4f^{14}5d]^2D_{7/2,5/2}$  states can be evaluated from  $|\Phi_0^{N+1}\rangle$  (denoted by  $|\Psi_a\rangle$ ). The point to be noted that the  $[4f^{14}6s^2]^2S_{1/2}$  state obtained from  $|\Phi_0^{N-1}\rangle$  and from  $|\Phi_0^{N+1}\rangle$  see different DF potentials. Consequently, the difference in the results of this state obtained using  $|\Psi_v\rangle$  and  $|\Psi_a\rangle$  at the same level of approximations may entail the effect of the 6s electron in the generation of the occupied orbitals.

Brief discussions on the approaches adopted to calculate  $|\Psi_v\rangle$  and  $|\Psi_a\rangle$  in the Fock-space RCC theory formalism are given here, but the detailed procedures can be found elsewhere [22, 23, 33], in which we express

$$|\Psi_v\rangle = e^{T^{N-1}} \{1 + S_v\} a_v^\dagger |\Phi_0^{N-1}\rangle \quad (7)$$

TABLE I: Contributions from the CCSD methods and comparison between the other available results of the quadrupole moments ( $\Theta$ ) in  $ea_0^2$  and the magnetic dipole hyperfine structure constant  $A_{hf}$  in MHz of the low-lying states relevant to the clock transitions in  $^{171}\text{Yb}^+$ .

RCC term	$4f^{13}6s^2\ ^2F_{7/2}$		$4f^{13}6s^2\ ^2F_{5/2}$		$4f^{14}6s\ ^2S_{1/2}$	$4f^{14}6s\ ^2D_{3/2}$		$4f^{14}6s\ ^2D_{5/2}$	
	$\Theta$	$A_{hf}$	$\Theta$	$A_{hf}$	$A_{hf}$	$\Theta$	$A_{hf}$	$\Theta$	$A_{hf}$
DF	-0.2593	867.66	-0.2097	1634.09	7390.40	2.503	290.33	3.694	110.50
$\overline{O}$ -DF	-0.0344	7.533	-0.0255	8.941	2547.16	-0.005	2.00	-0.008	1.13
$\overline{O}\Omega_1$	0.0	0.0	0.0	0.0	437.68	-0.431	54.83	-0.632	26.91
$\overline{O}\Omega_2$	0.0923	25.23	0.0715	87.47	2098.13	-0.022	16.28	-0.027	-212.29
$\Omega_1^\dagger\overline{O}\Omega_1$	0.0	0.0	0.0	0.0	5.01	0.047	4.73	0.056	1.58
$\Omega_1^\dagger\overline{O}\Omega_2$	0.0	0.0	0.0	0.0	-10.12	0.0003	3.80	-0.0002	-13.92
$\Omega_2^\dagger\overline{O}\Omega_2$	-0.0142	104.17	-0.0134	183.78	240.73	-0.024	28.31	0.033	17.16
Final	-0.216(20)	1004(100)	-0.177(50)	1914(166)	12709(400)	2.068(20)	401(14)	3.116(15)	-69(6)
Others	-0.22 <sup>a</sup> , -0.20 <sup>b</sup>				13091 <sup>b</sup>	2.174 <sup>c</sup>	489 <sup>b</sup>	3.244 <sup>c</sup>	-96 <sup>b</sup> , -12.58 <sup>c</sup>
						2.157 <sup>d</sup>	400.48 <sup>c</sup>		-48(15) <sup>e</sup>
Expt.	-0.041(5) <sup>f</sup> 905.0(5) <sup>g</sup>				12645 <sup>h</sup>	2.08(11) <sup>i</sup>	430(43) <sup>j</sup>		-63.6(5) <sup>k</sup>

<sup>a</sup>[20], <sup>b</sup>[21], <sup>c</sup>[17], <sup>d</sup>[18], <sup>e</sup>[12], <sup>f</sup>[9], <sup>g</sup>[26], <sup>h</sup>[27], <sup>i</sup>[19], <sup>j</sup>[28], <sup>k</sup>[29]

and

$$|\Psi_a\rangle = e^{T^{N+1}}\{1 + R_a\}a_a|\Phi_0^{N+1}\rangle, \quad (8)$$

where  $T^{N-1}$  and  $T^{N+1}$  excite core electrons from  $|\Phi_0^{N-1}\rangle$  and  $|\Phi_0^{N+1}\rangle$ , respectively, to account the electron correlation effects and the  $S_v$  operator annihilates the valence electron  $v$  that was appended by  $a_v^\dagger$  and creates a virtual orbital along with it carries excitations of the core electrons from  $|\Phi_0^{N-1}\rangle$  while the  $R_a$  operator creates the core electron  $a$  that was annihilated by  $a_a$  by creating a hole in another core orbital along with carrying excitations of the core electrons from  $|\Phi_0^{N+1}\rangle$ . As was mentioned before, the core orbitals of  $|\Phi_0^{N-1}\rangle$  do not see the interaction with the valence electron  $v$ . This effect along with the core-valence correlations are accounted through the contraction of  $T^{N-1}$  and  $\{1 + S_v\}a_v^\dagger$ . Analogously, the core electrons of  $|\Phi_0^{N+1}\rangle$  see extra effect from the spin pairing partner  $a$  which are removed through the product of  $T^{N+1}$  and  $\{1 + R_a\}a_a$ . Obviously, the core orbitals of  $|\Phi_0^{N+1}\rangle$  are more relaxed here. The singles and doubles excitations for the CCSD methods are denoted by defining  $T^L = T_1^L + T_2^L$  with  $L = N - 1$  or  $L = N + 1$  for the attachment and detachment cases, respectively,  $S_v = S_{1v} + S_{2v}$  and  $R_a = R_{1a} + R_{2a}$ . Contributions from the important triples are estimated perturbatively [23, 33] by contracting the DC Hamiltonian with  $T_2^{N-1}$  and  $S_{2v}$  in the electron attachment procedure and with  $T_2^{N+1}$  and  $R_{2a}$  in the detachment approach to estimate uncertainties due to the neglected triples.

The matrix element and the expectation value of a physical operator  $O$  between the  $|\Psi_f\rangle$  and  $|\Psi_i\rangle$  states

are determined in our RCC method by

$$\frac{\langle\Psi_f|O|\Psi_i\rangle}{\sqrt{\langle\Psi_f|\Psi_f\rangle\langle\Psi_i|\Psi_i\rangle}} = \frac{\langle\Psi_f|\{1 + \Omega_f^\dagger\}\overline{O}\{1 + \Omega_i\}|\Phi_i\rangle}{\sqrt{\mathcal{N}_f\mathcal{N}_i}}, \quad (9)$$

where  $\overline{O} = e^{T^{L\dagger}}Oe^{T^L}$  and  $\mathcal{N}_i = (1 + \Omega_i^\dagger)\overline{\mathcal{N}}(1 + \Omega_i)$  with  $\overline{\mathcal{N}} = e^{T^{L\dagger}}e^{T^L}$  for either  $L = N - 1$  or  $L = N + 1$  and  $\Omega_i$  is either  $S_i$  or  $R_i$ . Evaluation procedures of these expressions are described elsewhere [23, 33].

We present  $\Theta(\gamma J)$  values for all the considered states of  $^{171}\text{Yb}^+$  from our calculations and others calculations along with the  $A_{hf}$  results and compare them with the available measurements in Table I. We also give contributions from the DF method and from individual CCSD terms (complex conjugate (c.c.) contributions are given together) along with upper-bound uncertainties in the parentheses in the same table. As seen, our final  $\Theta$  values are almost in agreement with the other calculations and experimental results and are more precise, except for the  $\Theta$  value of the  $[4f^{13}6s^2]^2F_{7/2}$  state. Although calculations of Ref. [18] are carried out using the similar method of ours, but we have used a self-consistent procedure to account the contributions from the non-truncative  $\overline{O}$  series while in Ref. [18], terms are terminated at finite number of  $T^{N-1}$  operators. Our results for  $A_{hf}$  seem to be agreeing with the experimental values within their reported error bars, which are determined using  $g_I = 0.98734$  [34]. Here result for the  $[4f^{14}6s]^2S_{1/2}$  state is given from the electron detachment method, whereas electron attachment result can be found elsewhere [12]. We find difference between the results of the  $[4f^{14}6s]^2S_{1/2}$  state from these two approaches are

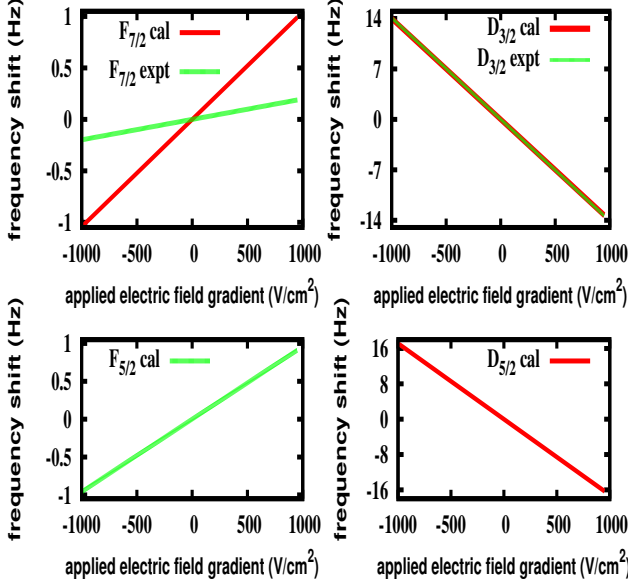


FIG. 2: (color online) Quadrupole shifts ( $\delta\nu$ ) in the  $[4f^{14}6s]^2S_{1/2}(F=0) \rightarrow [4f^{14}5d]^2D_{3/2}(F=2)$ ,  $[4f^{14}6s]^2S_{1/2}(F=0) \rightarrow [4f^{14}5d]^2D_{5/2}(F=2)$ ,  $[4f^{14}6s]^2S_{1/2}(F=0) \rightarrow [4f^{13}6s^2]^2F_{7/2}(F=3)$  and  $[4f^{14}6s]^2S_{1/2}(F=0) \rightarrow [4f^{13}6s^2]^2F_{5/2}(F=3)$  with  $M_F=0$  transitions against different electric field gradients ( $A$ ) using our calculated and measured  $\Theta$  values.

very significant and detachment theory gives more accurate result. Agreement between our  $A_{hf}$  result of the  $[4f^{13}6s^2]^2F_{7/2}$  state with its experimental value implies that our method is able to provide its wave function accurate enough indicating that its  $\Theta$  value can also be estimated in the similar accuracy. Therefore, the large differences between the theoretical and experimental results of  $\Theta$  of the  $[4f^{13}6s^2]^2F_{7/2}$  state are not being able to figured out evidently. Our intuitive guess is that this discrepancy could emanate, plausibly, from some unusual and unanticipated contributions arising through the triples or other higher excitations although such evidences were obscured from our study. This, therefore, calls for another experimental verification and more rigorous theoretical studies including higher level excitations to expunge the above ambiguity in the discrepancies between the theoretical and experimental results. Its value for the hyperfine  $[4f^{13}6s^2]^2F_{7/2}(F=3)$  state, in which state the actual measurement has been performed, yields as  $-0.19(2) ea_0^2$ . This value is almost same with the atomic  $\Theta$  value and again far away from  $-0.041(5) ea_0^2$  to assume that possibly it may correspond to  $\Theta$  of this hyperfine state. Considering our calculated  $\Theta$  values for all the states, we plot the quadrupole shifts ( $\delta\nu$ ) in the  $[4f^{14}6s]^2S_{1/2}(F=0) \rightarrow [4f^{14}5d]^2D_{3/2}(F=2)$ ,  $[4f^{14}6s]^2S_{1/2}(F=0) \rightarrow [4f^{14}5d]^2D_{5/2}(F=2)$ ,

$[4f^{14}6s]^2S_{1/2}(F=0) \rightarrow [4f^{13}6s^2]^2F_{7/2}(F=3)$  and  $[4f^{14}6s]^2S_{1/2}(F=0) \rightarrow [4f^{13}6s^2]^2F_{5/2}(F=3)$  transition frequencies against different  $A$  values and compare them against the results estimated using the available experimental  $\Theta$  values in Fig. 2. These results can be used to reduce the uncertainties in the clock transitions of  $\text{Yb}^+$  and for the further experimental investigations.

We also obtain M1 and E2 line strengths as  $2.5 \times 10^{-7}$  au and 110.25 au, respectively, for the  $[4f^{14}5d]^2D_{3/2} \rightarrow [4f^{14}6s]^2S_{1/2}$  transition from our calculation. Combining these values with the experimental energies, it yields  $A_{5d3/2 \rightarrow 6s}^{M1} = 2.07 \times 10^{-5} s^{-1}$  and  $A_{5d3/2 \rightarrow 6s}^{E2} = 19.70 s^{-1}$ . From these results, we get  $\tau_{5d3/2} = 50.78(50) ms$  which is in very good agreement with the experimental result  $52.7(2.4) ms$  of Ref. [10] and repudiate the argument by the latest experiment, which observes  $\tau_{5d3/2} = 61.8(6.4) ms$  [11], about underestimate of the systematics in the former measurement.

We acknowledge PRL 3TFlop HPC cluster for carrying out the computations.

---

\* Electronic address: dillip@prl.res.in; Electronic address: bijaya@prl.res.in

- [1] C. W. Chou et al., Phys. Rev. Lett. **104**, 070802 (2010).
- [2] W. H. Oskay et al., Phys. Rev. Lett. **97**, 020801 (2006).
- [3] K. Matsubara et al., Appl. Phys. Express **1**, 067011 (2008).
- [4] H. S. Margolis et al., Science **306** 19 (2004).
- [5] Chr. Tamm, S. Weyers, B. Lipphardt and E. Peik, Phys. Rev. A **80**, 043403 (2009).
- [6] M. Roberts et al., Phys. Rev. A **62**, 020501(R) (2000).
- [7] Y. Imai, K. Sugiyama, T. Nishi, S. Higashitani, T. Momiyama and M. Kitano, Poster No. B3-PWe21, *The 12th Asia Pacific Physics Conference*, 14-19 July, 2013.
- [8] N. Batra, S. De, A. Sen Gupta, S. Singh, A. Arora and B. Arora, arXiv:1405.5399 (2014).
- [9] N. Huntemann et al., Phys. Rev. Lett **108**, 090801 (2012).
- [10] N. Yu and L. Maleki, Phys. Rev. A **61**, 022507 (2000).
- [11] M. Schacht and M. Schauer, arXiv:1310.2530v1.
- [12] B. K. Sahoo and B. P. Das, Phys. Rev. A **84**, 010502(R) (2011).
- [13] S. Rahaman, J. Danielson, M. Schacht, M. Schauer, J. Zhang and J. Torgerson, arXiv:1304.5732.
- [14] S. Olmschenk et al., Phys. Rev. A **76**, 052314 (2007).
- [15] R. M. Godun et al., arXiv:1407.0164.
- [16] W. M. Itano, J. Res. Natl. Inst. Stand. Technol. **105**, 829 (2000).
- [17] W. M. Itano, Phys. Rev. A **73**, 022510 (2006).
- [18] K. V. P. Latha et al. Phys. Rev. A **76**, 062508 (2007).
- [19] T. Schneider, E. Peik, and C. Tamm, Phys. Rev. Lett. **94**, 230801 (2005).
- [20] P. J. Blythe, S. A. Webster, K. Hosaka, and P. Gill, J. Phys. B **36**, 981 (2003).
- [21] S. G. Porsev, M. S. Safronova and M. G. Kozlov, Phys. Rev. A **86**, 022504 (2012).
- [22] Y. Singh, B. K. Sahoo and B. P. Das, Phys. Rev. A **88**,

- 062504 (2013).
- [23] D. K. Nandy and B. K. Sahoo, Phys. Rev. A **88**, 052512 (2013).
  - [24] A. Szabo and N. Ostuland, *Modern Quantum Chemistry*, Dover Publications, Inc., Mineola, New York , First edition(revised), 1996.
  - [25] I. Shavitt and R. J. Bartlett, *Many-body methods in Chemistry and Physics*, Cambridge University Press, Cambridge, UK (2009).
  - [26] P. Taylor et al., Phys Rev. A **60**, 2829 (1999.)
  - [27] A. M. Martensson-Pendrill, D. S. Gough, and P. Hanaford, Phys. Rev. A **49**, 3351 (1994).
  - [28] D. Engelke, and C. Tamm, Europhys. Lett. **33**, 348 (1996).
  - [29] M. Roberts et al., Phys. Rev. A **60**, 2867 (1999).
  - [30] J. R. P. Angel, P. G. H. Sandars, and G. K. Woodgate, J. Chem. Phys. **47**, 1552 (1967).
  - [31] L. S. Brown and G. Gabrielse, Phys. Rev. A **25**, 2423(R) (1982).
  - [32] C. Schwartz, Phys. Rev. **97**, 380 (1955).
  - [33] B. K. Sahoo, S. Majumder, R. K. Chaudhuri, B. P. Das and D. Mukherjee, J. Phys. B **37**, 3409 (2006).
  - [34] N. J. Stone, Table of Nuclear Magnetic Dipole and Electric Quadrupole Moments, IAEA Nuclear Data Section, Vienna International Centre, Vienna, Austria, April (2011).